PHYSICAL REVIEW B **87**, 104103 (2013)

Effect of spatial redistribution of valence holes on the formation of a defect halo of swift heavy-ion tracks in LiF

N. A. Medvedev,[1,*] A. E. Volkov,[2,3,†] K. Schwartz,[4] and C. Trautmann[4]
[1]*TU Kaiserslautern and OPTIMAS Research Center, Erwin Schroedinger Str. 46, 67663 Kaiserslautern, Germany*
[2]*NRC Kurchatov Institute, Kurchatov Sq. 1, 123182 Moscow, Russia*
[3]*JINR, Joliot-Curie 6, 141980 Dubna, Moscow region, Russia*
[4]*GSI Helmholtz Centre, Planckstr.1, 64291 Darmstadt, Germany*

(Received 24 June 2012; revised manuscript received 6 January 2013; published 7 March 2013)

In-situ spectroscopy is applied to analyze the spatial distribution of point defects (F-color centers) formed in the nanometric vicinities of the trajectories of different swift heavy ions (from C to U) decelerated in LiF crystals in the electronic stopping regime. The formation of these defects results from the decay of self-trapped excitons appearing due to self-trapping and further relaxation of valence holes generated during beam induced ionization processes. A Monte Carlo model is applied to estimate the initial radial distribution of valence holes in the ion tracks by the time the ionization cascades are finished. It is demonstrated that there exists a large difference between this and the radial distribution of point defects detected in the experiments. This difference is described by fast and long-range diffusion of valence holes before their self-trapping. The effect illustrates the fundamental importance of the relaxation kinetics of the valence band on structure transformations in tracks. The average diffusion coefficient of holes D_h and their conversion efficiencies into color centers β in relaxing tracks of different ions in LiF are estimated ($D_h = 0.016$–$1.4\ \mathrm{cm}^2/\mathrm{s}$, $\beta = 0.01$–0.04).

DOI: 10.1103/PhysRevB.87.104103 PACS number(s): 61.82.Ms, 61.72.−y, 52.65.−y

I. INTRODUCTION

Swift heavy ions (SHI, $M \geqslant 10\, m_p$, where m_p is the proton mass) of the specific energy above about 1 MeV per nucleon (MeV/amu) deposit more than 90% of their kinetic energy into the electron subsystem of a solid. Depending on the projectile mass and energy, as well as on the target density, the electronic energy loss of such ions can reach up to several tens of kilo-electron-volts per nanometer along the ion path. Transfer of even a small part of the excess electronic energy into the lattice of a target can result in nanometric structure and phase transformations along the ion trajectory. The energy loss related to elastic scattering of such ions on target atoms is too low to induce the observed changes.[1,2]

The first step of SHI induced excitation of the electron subsystem of a solid results in the appearance of primary fast electrons (so-called δ electrons). Spatial spreading of these δ electrons and their collisions with valence and tightly bound electrons produce ionization cascades in the nanometric vicinity of the ion trajectory. The largest part of ionization cascades finishes by the time of ~10 fs[3–5] after the projectile passage. During this time, the initial radial distribution of valence holes, electronic vacancies in deep atomic shells, fast electrons in the conduction band, and other electronic excitations (e.g., excitons) are formed within an SHI track (in the following, we assume that the term "track" denotes a nanometric region of considerable material excitation along the ion trajectory).

The relaxation kinetics of the excess energy of the conduction band is usually taken into account in models of material excitation in tracks. For example, the two-temperature "thermal spike" model of lattice heating in SHI tracks[6–12] relies on a competition between the rate of decrease of the density of the electron energy in the conducting band due to spatial propagation of hot electrons (i.e., cooling down due to thermal conduction) and the transfer rate of a part of this energy into the lattice due to a difference between the lattice and electron temperatures.

The larger part of the excess energy of the electron subsystem in SHI tracks in insulators and wide band gap semiconductors is accumulated in electronic excitations originated from the valence band. Presently, there is a lack of models taking into account effects of the relaxation kinetics of the valence band on material excitations and structure transformations in relaxing SHI tracks. This paper provides a clear demonstration of the importance of these effects by presenting data and model calculations on the spatial redistribution of the excess energy of the valence band and the influence of this process on structural transformations in an SHI track.

We selected alkali-halides, in particular lithium fluoride crystals, as a model system for such a demonstration. Indeed, (i) these materials have the widest band gaps (14.6 eV in LiF) providing with an empty conduction band before an SHI irradiation. Any excitations of the electronic subsystem of alkali-halides (transient conduction band electrons, valence holes, excitons, etc.) in SHI tracks are originated from the valence band or deep atomic shell ionizations. (ii) In order to keep the electroneutrality of ionic crystals, point defects in alkali-halides have to trap charge carriers (electrons or holes) forming discrete energy levels for these carriers inside the band gap. This transforms point defects into color centers because transitions between these levels result in photon emissions. Detection of this emission by optical spectroscopy provides quantitative information about the concentration of point defects (color centers) and defect clusters,[13–15] i.e., information about structural changes in alkali halides. (iii) The relaxation of valence band based excitations can cause lattice damage in alkali halides. Indeed, in LiF, the potential energies of these excitations, e.g., of electron-hole pairs (>14.6 eV), excitons (13.6 eV), and self-trapped excitons

(4.8 eV), are larger than the energy of creation of a stable Frenkel pair of anion point defects comprised of an electron $F-$color center (an electron captured by an anion vacancy) and a hole $H-$color center (negative charged halogen molecule centered in an anion position).

The formation of self-trapped excitons provides the necessary localization of the excess electronic energy near an anion in alkali halides. Subsequent decay of such an exciton can stimulate formation of a pair of anion F- and H- color centers.[16,17] The emergence of a self-trapped exciton starts usually from the self-trapping of a valence hole (see also below).

(iv) The high mobility of valence holes in alkali-halides (e.g., their diffusion coefficient can reach the values of $D_h = 20\ \text{cm}^2/\text{s}$ in NaCl[18,19]) can result in large ranges of holes (10–100 nm) before their self-trapping within a picosecond time scale.[18,19]

With respect to SHI tracks, these mean that due to the fast spatial redistribution of valence holes before their self-trapping, the initial radial distribution of valence holes formed in a track within the time of the ionization cascades (~10 fs, radial extension ~100 nm[4,5]) cannot coincide with the spatial distribution of color centers appeared in tracks due to decay of self-trapped holes in the later stage. There is a chance to reveal this difference in experiments when the range of valence holes before their self-trapping is larger than the characteristic dimension of the initial distribution of holes in a track. The information about this difference will give us the ability to make quantitative conclusions about the kinetics of valence holes in a nanometric SHI track before their self-trapping, i.e., at the femto-pico-second timescales after the projectile passage.

Indeed, we detect in LiF crystals a large difference between the spatial distribution of color centers, measured in the *in-situ* spectroscopy experiments[14,15,20] in tracks of different ions (C, Ti, Au, U, Pb), and the initial radial distribution of valence holes calculated with the well tested Monte Carlo code. It is demonstrated that this difference occurs due to diffusion of valence holes before their self-trapping. An analysis of this difference allows us to estimate the key parameters governing the valence holes kinetics in tracks at the picosecond time scale: (a) the average diffusion coefficients of holes ($D_h = 0.016$–$1.4\ \text{cm}^2/\text{s}$) and (b) the conversion efficiency of valence holes into stable color centers ($\beta = 0.01 - 0.04$).

II. EXPERIMENT

Thin LiF platelets ($10 \times 10\ \text{mm}^2$) cleaved along one of (100) planes from a single crystal block grown from the melt in an inert atmosphere (Korth Kristalle, Germany) were used for irradiations (see Refs. 14 and 15 for details). The thicknesses of samples were between 0.2 and 0.5 mm. According to K_α x-ray emission spectra, the crystal contained about 20 ppm ($\sim 10^{18}\ \text{cm}^{-3}$) Mg and several ppm of Na and Cl trace elements.

The samples were exposed at room temperature to various ions (^{238}U, ^{208}Pb, ^{197}Au, ^{50}Ti, and ^{12}C) with the energies between 4 and 11 MeV/amu at the UNILAC linear accelerator of GSI. Irradiations with 2187 MeV Au ions and subsequent measurements without any heating of the samples were also performed at 8 K.[14,20]

The projectiles were slowing down in the electronic stopping regime, whereas elastic collisions of the ions with target atoms were important only at the very end of the ion paths (less than 1 μm) and gave only a negligible fraction of the ion induced damage. The projected ranges of all these ions in LiF were smaller than the sample thickness.[21]

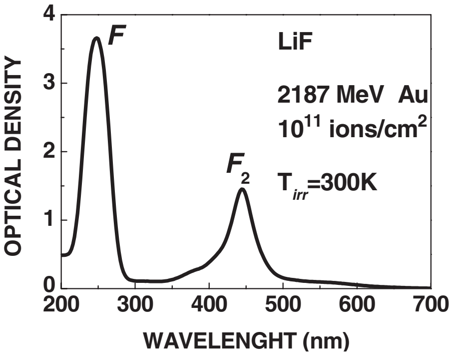

FIG. 1. The difference between the absorption spectra of a LiF crystal irradiated with 2187 MeV Au ion at 300 K and a virgin LiF crystal. The peaks of F- and F_2-color centers (two associated F centers) are presented.

The irradiations were performed under normal beam incidence with fluences (Φ) ranging from 10^9 to 10^{12} ions/cm^2. To avoid beam-induced heating of the samples, the ion flux was limited to 10^9 ions cm^{-2} s^{-1} for light ions (C) and to about 2×10^8 ions cm^{-2} s^{-1} for heavy ions. The ion flux was monitored with a secondary electron detector consisting of three 1-μm thick Al foils mounted in front of the sample and calibrated via the ion current in a Faraday cup (the inaccuracy $\leqslant 20\%$).[15]

The numbers of created F-centers in the irradiated LiF crystals were determined from the absorption spectra using a double beam Unicam UV4 spectrometer operating in the spectral range of 190–700 nm. The used samples are transparent for photons in this wavelength scale. F centers are characterized in LiF at room temperature by their absorption maximum at $\lambda_F = 250$ nm (see Fig. 1). The Smakula-Dexter formula $n_F = k \times D_{nF}$ links the concentration n_F of F-centers per cm^2 and the detected optical density D_{nF} $k = 9.48 \times 10^{15}$ and 6.08×10^{15} are the values for the room temperature and 8-K irradiations, respectively.[14,15,20]

The typical fluence dependence of the number of F-color centers n_F (Φ) per unit area detected in the irradiated samples is presented in Fig. 2. This dependence can be well fitted with the function

$$n_F(\Phi) = n_F^{\text{st}}\,[1 - \exp(-\Phi/\Phi_d)]. \qquad (1)$$

The fitting (1) assumes the following: (a) the initial linear dependence $n_F(\Phi) \approx n_F^{\text{st}}(\Phi/\Phi_d)$ of the concentration of color centers occurs at low fluences $\Phi \ll \Phi_d$ due to additive accumulation of defects generated in different tracks. The number ΔN_F of F centers produced in a single track can be estimated from the slope of the initial linear part of the dependence $n_F(\Phi)$ [see Eq. (1)]:

$$\Delta N_F = dn_F/d\Phi \approx n_F^{\text{st}}/\Phi_d, \qquad (2)$$

(b) The relaxation of defects (annihilation/aggregation) in the overlapping sections of neighboring tracks stimulates the deviation of $n_F(\Phi)$ from the linear dependence at $\Phi \geqslant \Phi_d$.

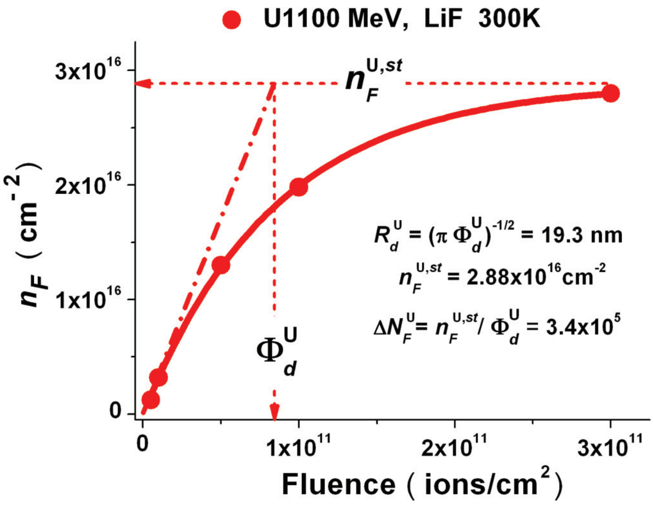

FIG. 2. (Color online) Fitting of the experimental dependence of the detected number of F-centers per unit surface area (n_{F}) on the fluence (Φ) for LiF crystals irradiated at room temperature with 1100 MeV U by Eq. (1). See explanation of the parameters n_F^{st} and Φ_d in the paper text.

The concentration of F centers saturates $[n_F(\Phi) \approx n_F^{\mathrm{st}}]$ when the track areas completely cover the sample surface at high fluences ($\Phi \gg \Phi_d$).

The fitting (1) assumes that all color centers created in a track are in the cylinder $r \leqslant R_d = (\pi\, \Phi_d)^{-1/2}$, which allows to estimate their average concentration there as

$$\langle C_F \rangle = \Delta N_F \left(\pi R_d^2 L\right)^{-1} = n_F^{\mathrm{st}}/L, \tag{3}$$

where L is the ion range. The value $\langle C_F \rangle$ can be treated as the threshold concentration necessary for stimulation of the intensive kinetics of F centers at the applied irradiation conditions and the parameters characterizing the transiently excited material in an SHI track.

Table I demonstrates an order of magnitude difference between the numbers of color centers ΔN_F produced in tracks of heavy and of light ions resulting from the large difference between the energies deposited by these ions into the electronic subsystem of the target. However, it is not a large difference in the values of the parameters R_d and $\langle C_F \rangle$ characterizing the radial distribution of color centers ("defect halo") in tracks of light and heavy ions. The average concentration $\langle C_F \rangle$ demonstrates the smallest variations. The color center kinetics depends very sharply on the achieved defect concentrations and on the realized values of the parameters characterizing transient material excitation in a track. The fitting model (1) assumes $\langle C_F \rangle$ as the threshold concentration for the initiation of intensive defect kinetics. It seems that the small differences between $\langle C_F \rangle$ indicate the similarity of parameters of the transiently excited material inside the cylinders $r < R_d$ for different ions.

III. MODEL

A two-step model is applied to describe the formation of the initial radial distribution of valence holes in a track during the time of their self-trapping (∼1 ps). At the initial times, which last before finishing of ionization cascades (∼10 fs after the projectile passage[4]), the Monte Carlo (MC) model of event-by-event simulations describes the excitation kinetics of the electron subsystem of a target due to inelastic scattering of a projectile as well as propagation, and elastic and inelastic scattering of fast electrons generated during ionizations of a target. The first version[3,4] of this MC model has been already successfully applied to the quantitative description of the x-ray spectroscopy experiments investigating emission from the highly ionized SHI track cores in $\mathrm{SiO_2}$. References 3 and 4 contain the theoretical basis as well as the details of this MC model and the numerical method used.

At first, the MC code simulates the ionizations of target atoms by a projectile resulting in the creation of the first generation of free electrons (δ electrons). Unlike Refs. 4 and 5, where the spatial distribution of target electrons was assumed according to their Bohr orbitals, the distribution of the positions of atomic electrons during a collision of an SHI with an atom is described in the new MC version by the relevant electron wave functions extracted from Ref. 22. Taking into account the large velocities of projectiles, the atomic electrons are assumed to be at the fixed positions during their energy and momentum exchange with an SHI (instant collisions). The momenta transferred to these electrons are calculated taking into account the impact parameters of the SHI relative to

TABLE I. The values of the parameters characterizing swift heavy projectiles, the spatial distribution of F centers, the conversion efficiencies of valence holes into stable Frenkel pairs, and the diffusion of valence holes before their self-trapping in tracks of different ions. S_e and L denote, respectively, the electronic energy loss and the range of an ion according to the SRIM-2008 code,[21] R_d is the effective radius of the defect halo, ΔN_F is the number of $F-$centers produced in a track, $\langle C_F \rangle$ is the average concentration of F centers in the defect halo, β is the portion of the initial valence holes transforming finally into stable F centers, and D_h is the averaged diffusion coefficient of valence holes in a track before their self-trapping.

Ion	E, MeV	S_e, keV/nm	L, μm	R_d, nm	ΔN_F, 10^4	$\langle C_F \rangle$, 10^{18} cm^{-3}	β	D_h, cm^{2}s^{-1}
C	58	0.6	63	9.1	6.8	4.1	0.04	0.034
C	133	0.3	246	5	4.6	2.4	0.013	0.016
Ti	555	3.4	117	10.9	9.3	2.16	0.01	0.14
Au (8 K)	2187	22.9	97.4	45.2	115	1.8	0.02	1.4
Au	2187	22.9	97.4	25.0	73	4.1	0.01	0.45
Pb	1600	25.3	67	22.8	62	5.7	0.01	0.44
Pb	2300	23.8	97	21.0	60	4.5	0.01	0.38
U	1100	32.6	45	19.3	34	6.4	0.008	0.48

the atomic nucleus.[3–5] Mutual interaction of atomic electrons during ionization of an atom by a projectile is not included in the presented version of the MC model, because this interaction affects only weakly the spectra of escaped electrons.[23]

Then, the MC code simulates the spatial propagation of the generated fast electrons and their elastic and inelastic scatterings on atoms resulting in the production of new free electrons and holes in different atomic shells. We stop tracing a free electron when its kinetic energy falls below the cut-off energy of $E_e^{\min} = 3E_{\text{gap}} \approx 40$ eV measured from the bottom of the conduction band. This energy corresponds to the experimentally detected energy of an incident electron necessary for the production of a stable pair of a conduction band electron and a valence hole in LiF.[16,24] The next generations of electrons are modeled in the same manner and the electron cascades are simulated event by event. The number of MC iterations was 10^4–10^5 depending on the achieved level of the initial excitation of the electronic subsystem in a track. Finally, the averaging over the obtained ensembles gives the radial distribution of holes in different atomic shells as well as the radial distribution of slow electrons with the energies lower than $E_e^{\min}$.

We do not take into account the creation of free excitons in the MC model because the experiments demonstrate that a fast electron decelerating in an alkali-halide crystal loses much less energy in creation of stable free excitons than in creation of stable electron-hole pairs: 5–10% versus 90–95% of the total energy losses of an electron, respectively.[16,25]

It should be noted that the main effects of electric fields appearing due to track ionizations on spatial redistribution of electrons are taken into account in the applied MC model. Indeed, charge screening is assumed in the used cross-sections describing scattering of electrons. This screening significantly reduces the effects of the fields.[26,27] Moreover, for fast electrons (with energies above several hundreds of electron volt), the effects of fields generated in a track can be neglected. The attracting field from the highly ionized track core (the region in the nearest vicinity of the ion trajectory) decelerates low-energy electrons flying apart. This attraction would decrease the region of electron spreading and, therefore, the region of creation of valence holes. Therefore accounting for effects of electric fields from the track core can only increase (slightly due to the screening) the difference between the calculated initial spatial distribution of valence holes and detected radial distribution of color centers in a track. This even strengthens the assumption about considerable spatial redistribution of valence holes before their self-trapping (see below).

The high mobility of valence holes[18,19] can result in their long-range spatial redistribution[28] during the times ranging from the stopping of ionization cascades to the time of hole self-trapping (0.5–1 ps, see Refs. 18 and 19). In the present paper, this spatial redistribution is modeled by the cylindrically symmetric diffusion equation

$$\frac{\partial C_h}{\partial t} = D_h \frac{1}{r}\frac{\partial}{\partial r}\left(r\frac{\partial C_h}{\partial r}\right). \tag{4}$$

Here, C_h is the concentration of holes and D_h is their diffusion coefficient. Taking into account the large difference between the time of finishing of ionization cascades (∼10 fs) and the time of self-trapping of valence holes (∼1 ps) we assume the distribution of valence holes obtained from the MC simulations as the initial condition for the diffusion problem (4).

Concentrating on a demonstration of a possibility of a large spatial redistribution of holes before their self-trapping and in order to simplify the diffusion problem (4), we use in this paper the constant values D_h averaged temporally and spatially. These values of D_h are extracted for different ions by a fitting based on the comparison of the calculated initial radial distribution of valence holes by the time ionization cascades are finished with the radial distribution of F centers detected in experiments. Of course, the average value of the diffusion coefficient D_h depends on the irradiation conditions (e.g., the irradiation temperature). It also depends on the values of the parameters characterizing the transient state of the excited material in a track (e.g., the transient electronic and lattice temperatures). Thus the values of D_h are different in tracks of different ions. We assume also that all possible effects of generated electric fields on diffusion of holes are taken into account by this average value D_h, so the coefficient D_h can be treated as the mean ambipolar-diffusion coefficient.

Moreover, the fitted value D_h considers also a possible effect of diffusion of free excitons because the motion of excitons and their self-trapping are controlled by the slow motion of their massive hole component ($m_h = 3.5\, m_e$).[16] This allows taking into account the effect of free excitons in the diffusion model (4) as a little decrease of the averaged diffusion coefficient of valence holes. It is not necessary to calculate this little correction because D_h is the fitting parameter of the model.

The general solution of Eq. (4) with the initial radial distribution of valence holes $C_h(r,0) = C_0^h(r)$ is given by the formula [29]

$$C_h(r,t) = \frac{1}{2D_h t}\exp\left(-\frac{r^2}{4D_h t}\right) \times \int_0^\infty \xi\, d\xi\, C_0^h(\xi)\exp\left(-\frac{\xi^2}{4D_h t}\right) I_0\left(\frac{r\xi}{2D_h t}\right), \tag{5}$$

where $I_0(x)$ is the modified Bessel function of the first kind. By the time the self-trapping of valence holes occurs, the solution of Eq. (5) gives, taking into account the conversion efficiency of holes into defects (see Sec. IV A), the parameters of the initial radial distribution of color centers formed due to the decay of self-trapping holes/excitons. It is demonstrated in Sec. IV C that thermally activated diffusion of color centers as well as diffusion of self-trapped holes changes negligibly this initial distribution of defects before the spectroscopy measurements.

IV. RESULTS AND DISCUSSION

A. Efficiency and the basic mechanism of conversion of valence holes into color centers in SHI tracks

The temporally and spatially averaged conversion efficiency β of a valence hole into a stable Frenkel pair of color centers can be estimated by a comparison of the number ΔN_F of F centers produced in a single track [see Eq. (2)] with the calculated total number of valence holes generated there (see Fig. 3). Depending on the parameters of the excited material in a track, the values of β range from 0.008 to 0.04 for different ions (see Table I) and agree reasonably well with $\beta \approx 0.05$ measured for LiF in the synchrotron irradiation experiments.[16]

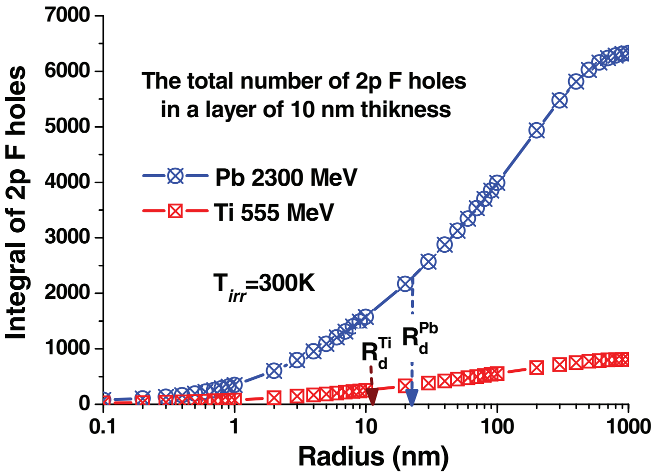

FIG. 3. (Color online) The calculated initial number of valence holes contained in the cylinder of the thickness of 10 nm and the radius r centered at the track axis by the time the ionization cascades are finished (10 fs after the projectile passage).

The inaccuracy of the obtained values β is determined mainly by the inaccuracy of the fluence/flux measurements in the irradiation experiments (~20%).

These low conversion efficiencies ($\beta \ll 1$) demonstrate that only a small part of the initial valence holes is finally converted into stable color centers during relaxation of the excess energy of the electron-hole pairs in SHI tracks in alkali halides. The larger portion of the excess energy contained in electron-hole pairs relaxes without formation of Frenkel pairs in these materials. Radiative decay is the most efficient channel of such relaxation when no point defects are formed. Also, the high transient concentration of electron-hole pairs in the nearest vicinity of the projectile trajectory ($r < 1$ nm) provides a characteristic time of the Auger-like processes (three-particles recombination) comparable or shorter to that of the radiative decay of these pairs.[4]

The creation of a Frenkel pair of color centers in alkali-halides during the relaxation of an electron-hole pair needs a prior localization of the excess electronic energy in the close vicinity of a halogen atom. The most effective mechanism of such spatial localization is realized by means of formation of a self-trapped anion exciton (STE)[30] whose energy level in LiF is located within the gap at 4.8 eV from the top of the anion valence band.

The formation of a self-trapped anion exciton can be realized via two channels. The first one starts from the formation of a free exciton (13.6 eV from the top of the anion valence band in LiF) followed by the formation of a self-trapped exciton. The second channel originates from the initial formation of a self-trapped anion hole and its subsequent relaxation with a conduction band electron resulting in the formation of a self-trapped exciton.

A fast electron decelerating in an alkali-halide crystal loses a little part of its energy on the creation of stable free excitons.[16,25] Therefore the initial concentration of free excitons in a track is negligible in comparison to the concentration of valence holes by the time the ionization cascades are finished. Moreover, the time of a free exciton creation stimulated by relaxation of a primary created electron-hole pair should be larger than the self-trapping time of a valence hole. Indeed, according to the Einstein formula,[31] the characteristic time of spontaneous decays of a quantum system is inversely proportional to the third power of the energy released in these processes ($\sim E^{-3}$). When the excess energy of an electron-hole pair in LiF is relaxing, the minimal energy released during the creation of a self-trapped hole (3.8 eV in LiF) is four times larger than the energy released when a free exciton is formed (14.6–13.6 eV = 1 eV in LiF). The low energy cost results in the weak intensity of free exciton formations during spontaneous decay of an electron-hole pair. Taking these arguments into account, one can conclude that the probabilities of free exciton creation are low for both, collision events (the small cross section) and spontaneous decays (the energy cost).

B. Effect of spatial spreading of fast electrons on the formation of the initial radial distribution of valence holes

Figure 4 presents the calculated initial radial distribution of the concentration $C_0{}^h(r)$ of holes created in the 10-nm thickness layer with the axis coinciding with the SHI trajectory (Pb 2300 MeV) by the time the ionization cascades are finished (~10 fs after the projectile passage[4]). This radial dependence consists of two segments. The weak initial radial dependence of the valence hole concentration $C_0{}^h(r) \sim 1/r^{1.3}$ is observed in the central track region $r < R_c = 2$–3 nm. Approximately 30% of the valence holes are created in this region (see Fig. 3) resulting in their extremely high initial volume density there. The particular value of the radius R_c depends on the threshold energy $E_e^{\min}$ (see above). The used value $E_e^{\min} = 3E_g \approx 40$ eV results in $R_c = 2$–3 nm for different ions. This radius increases to up to $R_c \approx 10$ nm when $E_e^{\min} = 10$ eV, similarly to Ref. 26.

The initial concentration of valence holes decreases as $C_0{}^h(r) \sim 1/r^{1.9}$ at distances $R_c < r < R_s$ from the projectile trajectory (the values of R_s range from 200 to 500 nm for different ions). This dependence is very close to, but does not coincide with the inverse square dependence ($\sim 1/r^2$). The importance of this difference for an application of the

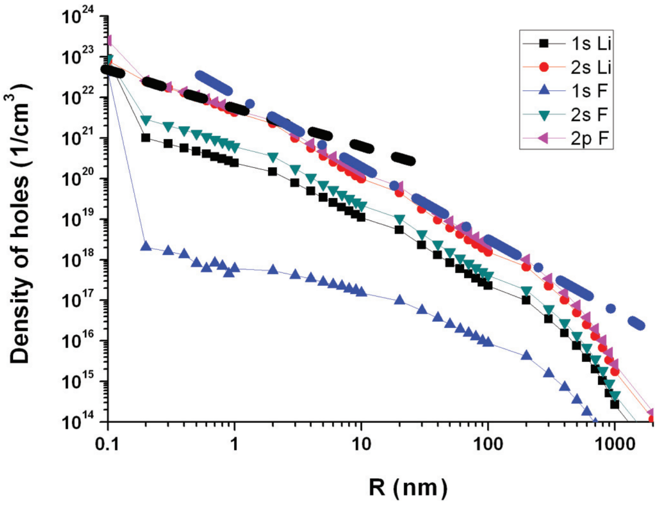

FIG. 4. (Color online) The initial radial distribution of holes by the time all ionization cascades are finished (10 fs) in the vicinity of the trajectory of Pb-ion ($E = 2300$ MeV) in a LiF crystal.

diffusion model of spatial redistribution of holes before their self-trapping will be discussed below.

A partitioning of the initial radial distribution of the excess energy deposited into the electronic subsystem in SHI tracks was also noticed by the authors of Refs. 26–28,32. It was shown in Refs. 26 and 28 that, similar to our results, the radial distribution of the excess energy of the electronic subsystem deviates considerably from the r^{-2} dependence at short distances ($r < R_c \approx 10$ nm if $E_e^{\min} = 10$ eV). In Ref. 28, the spatial distribution of the excess energy of the electronic subsystem is modeled by the constant value in this region. The mechanisms of formation of this dependence were not discussed there. The radial distribution of the excess energy of the electron subsystem in SHI tracks similar to $1/r^2$ was confirmed in a number of experiments on irradiations of gaseous targets.[33,34] It should be noted that a little deviation of the radial distribution of the deposited energy from the r^{-2} dependence at distances $r > R_c$ was also noted in Refs. 27 and 28.

Valence holes are generated in ionization cascades produced by fast electrons. The appearance of the two main segments in the initial radial distribution of valence holes can be described by the existence of two processes governing spatial spreading of these electrons from the SHI trajectory: (a) the ballistic spreading, when collisions change the momentum of a fast electron only slightly, and (b) the diffusion, when frequent collisions result in chaotic and considerable changes of the momentum of a moving electron.[4]

The emergence of ($\sim 1/r^2$) dependence was described in Ref. 26 by the constant deceleration rate of ballistic δ-electrons moving away from the SHI trajectory or, more exactly, when the Rutherford cross section (small angle scattering) was applied to describe the collision kinetics of these electrons.[26–28,35] For high-energy electrons (>180 eV according to Ref. 28), the ballistic motion dominates forming a radial dependence of the density of ionized states very close to the inverse square one at distances $r > 2$–3 nm from the ion trajectory. A deviation of the initial radial distribution of valence holes in this region from the inverse square one ($\sim 1/r^k$, $k \approx 1.9 \neq 2$) results from a little contribution of the diffusion process in the spatial propagation of fast electrons[5] (rear events with considerable momentum transfer).

The radial dependence of the concentration of valence holes deviates from the above mentioned dependencies in the immediate vicinity of the ion trajectory ($r < 2$ Å) where material ionization is produced by a projectile directly. *On-line* x-ray spectroscopy experiments[36] provided to us information about the relaxation kinetics of the highly ionized region in the immediate vicinity of the ion trajectory ($r < 2$ Å). This information was used to test the developed MC model of excitation of the electronic subsystem in SHI tracks (see Refs. 3 and 4).

Figure 4 demonstrates that fast electrons create also valence holes at large distances ($r \geqslant 500$ nm) from the ion trajectory forming the outer part of the region affected by a projectile. This region accumulates a negligible part of generated valence holes and affects insignificantly the number of detected color centers. However, the effects of these regions can be observed in experiments. Indeed, overlapping of these outer regions from neighboring tracks occurs at low fluences $(0.5-1) \times 10^8$ cm^{-2}. These fluences coincide with the incubation fluences Φ_{inc} providing the initial changes of the optical properties of alkali halides irradiated with SHIs (e.g., bleaching).[14,20] These changes can be ascribed to a neutralization of trace elements by free carriers (holes and electrons). Therefore we can conclude that the incubation fluence corresponds to the overlap of the outer regions of electronic excitations from different ions.

It should be noted that rare ionization events in the electronic subsystem at large distances from the SHI trajectory lead to rather large statistical fluctuations in realizations of the numerical algorithm. In order to reduce these fluctuations, we introduced in the MC model a logarithmic scale for the radial distribution of electron and hole densities. In this case, a low number of ionization events is partly compensated by a larger volume, over which the density is defined. This significantly reduces the number of MC iterations necessary to obtain smooth distributions.

C. Spatial redistribution of valence holes before their self-trapping

Analysis of the calculated initial radial distribution of valence holes by the time the ionization cascades are finished ($\leqslant 10$ fs, see Ref. 4) demonstrates that, even if we take into account the largest conversion efficiency $\beta \approx 0.04 \ll 1$, the initial concentration of holes is too low at distances $r > 5$ nm from the ion trajectory and too high in the central track region in order to reproduce the parameters R_d and $\langle C_F \rangle$ of the radial distribution of F centers detected in the experiments (see Fig. 5). The following mechanisms could be assumed to describe the difference between parameters of the calculated initial radial distribution of valence holes and the detected radial distribution of color centers in an SHI track: (a) fast spatial redistribution of valence holes in the vicinity of the ion trajectory before their self-trapping ($\tau = 0.5$–1 ps), (b) diffusion of formed defects before the spectroscopy measurements, and (c) diffusion of self-trapped holes before their decay. As discussed below, only diffusion of valence holes can be responsible for this difference.

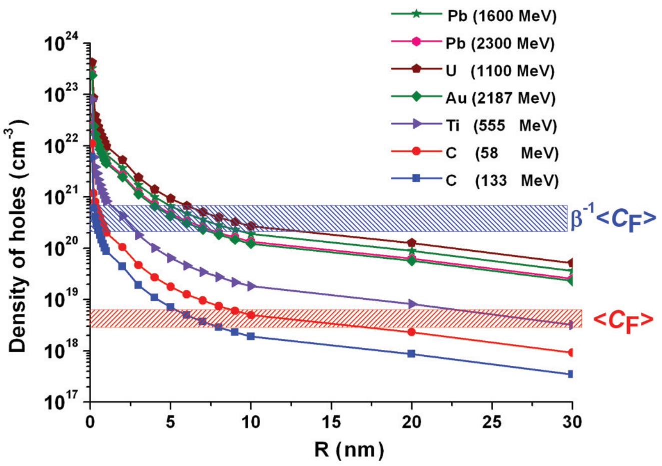

FIG. 5. (Color online) Comparison between the calculated initial concentrations of valence holes and the concentrations $\langle C_F \rangle$ ($\beta^{-1}\langle C_F \rangle$) of detected F centers averaged over the defect halo (hatched areas) in irradiated LiF crystals. R is the radial distance from the ion trajectory. $\beta = 0.008$–0.04 is the portion of the initial valence holes transforming finally into F centers (see Table I).

First of all, this conclusion is confirmed by the difference between the radial distributions of holes and color centers observed in the cryogenic (8 K) irradiations of LiF with 2187 MeV Au ions, when the negligible diffusion lengths of point defects are dramatically insufficient to form the detected radius of the defect distribution. Indeed, Ref. 14 demonstrates that the diffusion of even the faster *H*- and *I*-interstitial color centers is frozen in SHI tracks in LiF crystals irradiated at 8 K.

Of course, the increase of the irradiation temperature from 8 to 300 K intensifies the defect kinetics in a relaxing track in alkali halides (aggregation and recombination, see Refs. 14 and 20 for details). In particular, the temperature stimulated defect kinetics results in a decrease of the number ΔN_F of *F* centers remained in a track after its cooling down ($\Delta N_F = 115 \times 10^4$ at 8 K versus $\Delta N_F = 73 \times 10^4$ at 300 K for Au 2187 MeV, see Table I) as well as in the smaller radius R_d of the region containing the kinetically active defect concentration (R_d (8 K) = 45.2 nm versus R_d (300 K) = 25.0 nm for Au 2187 MeV, see Fig. 6). However, such increase of the temperature can accelerate diffusion of only *H* centers.[14] Due to the high value of the migration barrier of *F* centers in LiF ($U_{\mathrm{F}} = 1.5$ eV, Refs. 37 and 38), their diffusion is frozen up to temperatures ≈420 K (see Ref. 14). Therefore the low heating (∼100 K) of SHI track in LiF detected in Ref. 14 and confirmed by calculations (see Ref. 39) cannot explain the difference between the initial radial distribution of valence holes and the radial distribution of *F*-color centers detected by spectroscopy measurements in LiF crystals irradiated at room temperature.

The high ionization density, which can occur at the initial stage of track relaxation, may cause a transient modification of the interatomic potential in the close vicinity of the SHI trajectory. This can stimulate a transient decrease of the diffusion barrier of color centers or may even cause nonthermal melting of the lattice there.[40,41] To the best of our knowledge, there are no data about the diffusion barrier of *F* centers in the highly ionized lattice of LiF. For an estimation, we use the lowest reported value of the barrier realized for photoexcited *F* centers (F^* centers) in alkali halides (0.2 eV in KCl, KBr, which is comparable to the diffusion barrier of *H* and *I* centers).[42,43] But even for this extremely low diffusion barrier, the short transient state of the ionized lattice (10^{-14}–10^{-11}s) would result in diffusion lengths of *F* centers too short to describe the observed difference between the radial distribution of valence holes and the radial distribution of *F* centers detected in a track. The diffusion coefficient of self-trapped holes is also too low[18,30] to provide the necessary long distance diffusion before their decay.

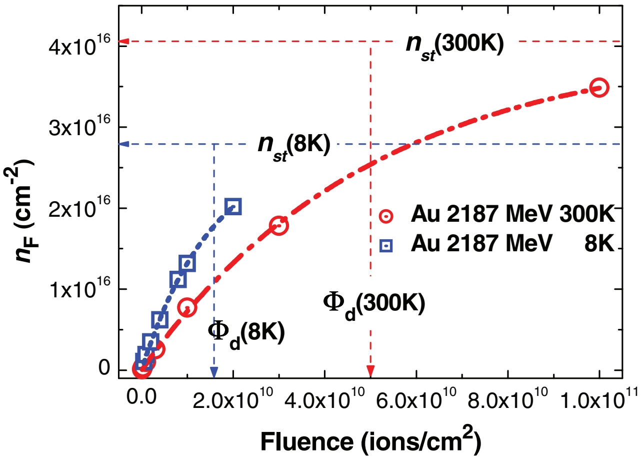

FIG. 6. (Color online) The dependencies of the detected number of *F* centers per unit surface area (n_{F}) on the fluence (Φ) for LiF crystals irradiated with 2187 MeV Au ions at room temperature and at 8 K.

Finally, conversion of even only 1% of the initial valence holes into Frenkel pairs would result in a concentration of *F* centers $C_F > 10^{21}$ cm^{-3} in the central track region ($r \leqslant 3$ nm). Effects of such extremely high defect concentration would be detected in experiments (defect aggregates, amorphization, phase explosion, etc.). However, LiF crystals demonstrate no amorphization or other considerable structure and phase transformations under SHI irradiation at fluencies investigated in this work. Taking into account the low diffusivity of color centers, this can be described by fast escape of valence holes from the central region of an SHI track.

Therefore based on the argumentation above, we can conclude that the fast spatial redistribution of valence holes before their self-trapping governs the formation of the initial radial distribution of defects (the "defect halo") in SHI tracks in the irradiated LiF crystals.

As it was demonstrated above, the initial radial distribution of holes obtained in the MC simulations by the time the ionization cascades are finished has the following form:

$$C_0(r) = \frac{C_0 R_0^k}{r^k}\ , \tag{6}$$

where $k = k_1 \approx 1.3$ when $r < R_c \approx 2$–3 nm, and $k = k_2 \approx 1.9 < 2$ when $r > R_c$. This initial distribution (6) results in the following form of the solution (5) of the diffusion equation (4) (see Ref. 44):

$$\begin{aligned} C_h(r,t) &= C_0\left(\frac{R_0^2}{4D_h t}\right)^{k/2}\Gamma(1-k/2)\exp\left(-\frac{r^2}{4D_h t}\right)\\ &\quad\times {}_1F_1\left[(1-k/2);1;\frac{r^2}{4D_h t}\right]\\ &= \frac{2^{1-n}C_0\Gamma(1-k/2)}{4k(D_h t)^{n/2+1}}\exp\left(-\frac{r^2}{4D_h t}\right)\\ &\quad\times\left[(2kD_h t - r^2)L^0_{k/2}\left(\frac{r^2}{4D_h t}\right) + r^2 L^1_{k/2}\left(\frac{r^2}{4D_h t}\right)\right], \end{aligned} \tag{7}$$

where $\Gamma(x)$ is the Gamma function,

$$\begin{aligned} {}_1F_1(\alpha;\gamma;z) &= \sum_0^\infty \frac{(\alpha)_m}{(\gamma)_m} z^m\ ,\\ (a)_m = a(a+1)\ldots(a+m-1) &= \frac{\Gamma(a+m)}{\Gamma(a)} \end{aligned} \tag{8}$$

is the confluent hypergeometric function, and

$$\begin{aligned} L_n^\lambda(z) &= \frac{(\lambda+1)_n}{n!}\,{}_1F_1(-n;\lambda+1;z)\\ &= \frac{(\lambda+n)!}{\lambda!n!}\,{}_1F_1(-n;\lambda+1;z) \end{aligned} \tag{9}$$

is the generalized Laguerre function of a degree n and index λ[45].

The following relations are used in Eq. (7):

$$ {}_1F_1\left[(1-k/2);1;\frac{r^2}{4D_h t}\right] = L^0_{k/2-1}\left(\frac{r^2}{4D_h t}\right), \qquad (10)$$

$$ (n+\lambda)L^{\lambda}_{n-1}(z) = zL^{\lambda+1}_n(z) + (n-z)L^{\lambda}_n(z). \qquad (11)$$

As mentioned above, the little deviation of the radial dependence of the initial spatial distribution of valence holes from the inverse square one ($\sim 1/r^k$, $k \approx 1.9 \neq 2$) results from a small contribution of the diffusion to the spatial spreading of fast electrons in a track. Nonetheless, this little deviation from the $\sim 1/r^2$ dependence has a significant importance for the application of the diffusion model [see Eq. (4)] to the description of spatial redistribution of valence holes. Indeed, for $D_h = \text{const}$, the real solution (7) of Eq. (4) with initial conditions (6) exists only for $k < 2$ (see Ref. 45). Therefore the initial conditions based on the inverse square dependence (or higher, $k \geqslant 2$) cannot be used for modeling of diffusion of holes from the ion track. In this case ($k \geqslant 2$, e.g., Ref. 27), a short temporal mesodiffusion stage[46] should be taken into account to interpret a fast transition of the initial radial distribution of holes into that providing the appearance of the diffusive behavior in their spatial spreading.

The radial distributions (7) of the concentration of valence holes in SHI tracks obtained from the solution of the diffusion equation (4) with the initial condition (6) corresponding to the outer region $r > R_c = 2$–3 nm of the initial radial distribution of valence holes resulted from MC simulations ($k = k_2 \approx 1.9$, see Fig. 4) are presented in Fig. 7 for different times after the projectile passage (Au 2187 MeV). Figure 7 demonstrates that the solution (7) tends quickly to a plateaulike radial distribution of the concentration whose height decreases with time. It is worth to note that the plateaulike radial distributions of valence holes are favorable for using the averaged parameters $\langle C_F \rangle$ and R_d characterizing the spatial distribution of defects in the vicinity of the SHI trajectory as well as the averaged conversion efficiency of holes β in the estimations made in this paper.

To the best of our knowledge, there are no data available for the diffusivity of valence holes in strongly excited nanometric SHI tracks in alkali halides. However, this diffusivity can be estimated by fitting of the experimentally detected effective radius R_d of the spatial distribution of F centers with the diffusion length of valence holes (7) by the time of their self-trapping ($\tau_{\text{st}} = 0.5$–1 ps). The conversion efficiency $\beta \ll 1$ ($\langle C_F \rangle \beta^{-1}$) must be taken into account in such a fitting. The estimated values of the averaged diffusion coefficients D_h of valence holes are collected in Table I demonstrating that D_h ranges from 0.1 cm^2/s to 1.4 cm^2/s in tracks of different ions. These values are much larger than the diffusion coefficients of color centers ($U_{\text{F}} = 1.5$ eV, Refs. 37 and 38) and self-trapped holes (see Refs. 18 and 30). As it was mentioned above, the values of the effective diffusion coefficients of holes D_h depend on the irradiation conditions and the values of the parameters characterizing the transient states of excited electronic and ionic subsystems realized in tracks of different ions.

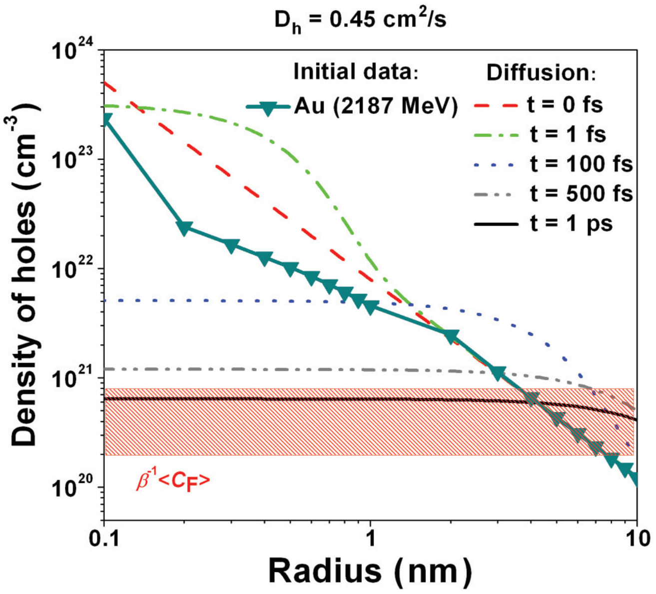

FIG. 7. (Color online) Build-up of the plateaulike form of the radial dependence of the concentrations of valence holes in a track of Au 2187 MeV ion, resulting from the solution (7) of the diffusion problem (4). The used initial condition corresponds to the outer region $r > R_c = 2$–3 nm of the initial radial distribution of valence holes resulted from MC simulations ($k = k_2 \approx 1.9$).

V. CONCLUSIONS

The importance of the relaxation kinetics of the valence band on structure transformations in SHI tracks is demonstrated by the effect of fast long-range spatial redistribution of valence holes on the creation of the ensemble of point defects (color centers) in SHI tracks in LiF. The values of the key parameters governing the kinetics of valence holes in a relaxing SHI tracks in LiF at the picosecond time scale after the projectile passage were estimated, and they are (a) the average diffusion coefficient of valence holes ($D_h = 0.016$ – 1.4 cm^2/s) and (b) the conversion efficiency of valence holes into color centers ($\beta = 0.01$–0.04).

ACKNOWLEDGMENTS

The financial supports from Russian Foundation for the Basic Research (Grants 11-08-90424 Ukr-f-a, 11-08-91162 GFEN-a) as well as from Deutsche Forschungsgemeinschaft (Grant TR 973/1-1) and Helmholtz Association (Grant IK-RU-002) are acknowledged.

---

[*] Present address: CFEL at DESY, Notkestr. 85, 22607 Hamburg, Germany.

[†] Corresponding author: a.e.volkov@list.ru

[1] F. F. Komarov, Phys. Usp. **46**, 1253 (2003).

[2] N. Itoh, D. M. Duffy, S. Khakshouri, and A. M. Stoneham, J. Phys.: Condens. Matter **21**, 474205 (2009).

[3] N. A. Medvedev, A. E. Volkov, B. Rethfeld, and N. S. Shcheblanov, Nucl. Instrum. Methods Phys. Res. B **268**, 2870 (2010).

[4] N. A. Medvedev, A. E. Volkov, N. S. Shcheblanov, and B. Rethfeld, Phys. Rev. B **82**, 125425 (2010).

[5] O. Osmani, N. Medvedev, M. Schleberger, and B. Rethfeld, Phys. Rev. B **84**, 214105 (2011).

[6] V. L. Ginzburg and V. R. Shabanskiy, Dokl. Akad. Nauk SSSR **100**, 445 (1955).

[7] M. I. Kaganov, I. M. Lifshitz, and L. V. Tanatarov, Sov. Phys. JETP **4**, 173 (1957).

[8] Yu. V. Martynenko and Yu. N. Yavlinskii, Atomnaya Energiya **62**, 80 (1987).

[9] M. Toulemonde, C. Dufour, and E. Paumier, Phys. Rev. B **46**, 14362 (1992).

[10] G. Szenes, Phys. Rev. B **51**, 8026 (1995).

[11] A. E. Volkov and V. A. Borodin, Nucl. Instrum. Methods Phys. Res. B **146**, 137 (1998).

[12] V. P. Lipp, A. E. Volkov, M. V. Sorokin, and B. Rethfeld, Nucl. Instrum. Methods Phys. Res. B **269**, 865 (2011).

[13] A. Meftah, F. Brisard, J. M. Costantini, M. Hage-Ali, J. P. Stoquert, F. Studer, and M. Toulemonde, Phys. Rev. B **48**, 920 (1993).

[14] K. Schwartz, A. E. Volkov, M. V. Sorokin, C. Trautmann, K.-O. Voss, R. Neumann, and M. Lang, Phys. Rev. B **78**, 024120 (2008).

[15] K. Schwartz, A. E. Volkov, M. V. Sorokin, R. Neumann, and C. Trautmann, Phys. Rev. B **82**, 144116 (2010).

[16] Ch. B. Lushchik, in *Physics of Radiation Effects in Crystals*, edited by R. A. Johnson and A. N. Orlov (North-Holland, Amsterdam, 1986), pp. 473–526.

[17] N. Itoh, A. M. Stoneham, *Materials Modification by Electronic Excitations* (Cambridge University Press, Cambridge, 2001).

[18] M. Elango, Radiat. Eff. Defects Solids **128**, 1 (1994).

[19] K. Tanimura and W. P. Hess, Phys. Rev. B **69**, 155102 (2004).

[20] K. Schwartz, M. Lang, R. Neumann, M. V. Sorokin, C. Trautmann, A. E. Volkov, and K.-O. Voss, Phys. Status Solidi C **4**, 1105 (2007).

[21] J. F. Ziegler, J. P. Biersack, and U. Littmark, *The Stopping and Range of Ions in Solids* (Pergamon Press, New York, 1985, new edition in 2009), p. 321; http://www.srim.org.

[22] P. L. Grande and G. Schiwietz, Nucl. Instrum. Methods Phys. Res. B **195**, 55 (2002).

[23] A. A. Baranov, N. A. Medvedev, A. E. Volkov, and N. S. Scheblanov, Nucl. Instrum. Methods Phys. Res. B **286**, 51 (2012).

[24] Ch. B. Lushchik and A. Ch. Lushchik, *Decay of Electronic Excitations with Defect Formation in Solids* (Nauka, Moscow, 1989), p.104.

[25] E. A. Vasil'chenko, Ch. B. Lushchik, and K. Osmonaliyev, Sov. Solid State Phys. **28**, 1113 (1986).

[26] M. P. R. Waligorski, R. N. Hamm, and R. Katz, Nucl. Tracks Radiat. Measur. **11**, 309 (1986).

[27] A. Akkerman, M. Murat, and J. Barak, Nucl. Instrum. Methods Phys. Res. B **269**, 1630 (2011).

[28] M. Martini, G. Spinolo, and A. Vedda, Il Novo Cimento **3**, 1017 (1984).

[29] B. M. Budak, A. A. Samarski, and A. N. Tikhonov, *A Collection of Problems on Mathematical Physics*, International Series of Monographs in Pure and Applied Mathematics, Vol. 52 (Pergamon Press, Oxford, 1964).

[30] K. S. Song and R. T. Williams, *Self-Trapped Excitons* (Springer-Verlag, Berlin, 1996), p. 410.

[31] L. D. Landau and L. M. Lifshitz, *Quantum Mechanics Non-Relativistic Theory*, 3rd ed. (Butterworth-Heinemann, Amsterdam), Vol. 3, p. 691.

[32] P. Martin, S. Guizard, P. Daguzan, G. Petite, P. D. Oliveira, P. Meynadier, and M. Perdrix, Phys. Rev. B **55**, 5799 (1997).

[33] G. Laczko, V. Dangendorf, M. Kramer, D. Schardt, and K. Tittelmeier, Nucl. Instrum. Methods Phys. Res. A **535**, 216 (2004).

[34] T. Elsasser, R. Cunrath, M. Kramer, and M. Scholz, New J. Phys. **10**, 075005 (2008).

[35] F. A. Cucinotta, R. Katz, J. W. Wilson, and R. R. Dubey, NASA Technical Memorandum **3497**, 1 (1995).

[36] J. Rzadkiewicz, O. Rosmej, A. Blazevic, V. P. Efremov, A. Gojska, D. H. H. Hoffmann, S. Korostiy, M. Polasik, K. Slabkowska, and A. E. Volkov, High Energy Density Phys. **3**, 233 (2007).

[37] D. Binder and J. Sturm, Phys. Rev. **99**, 603 (1955).

[38] A. P. Surzhikov, A. V. Chernyavskii, A. Ghyngazov, and T. S. Franglyan, Russ. Phys. J. **45**, 1190 (2002).

[39] S. A. Gorbunov, N. A. Medvedev, P. N. Terekhin, and A. E. Volkov, Phys. Status Solidi C (2013), doi: 10.1002/pssc.201200875.

[40] A. Rousse, C. Rischel, S. Fourmaux, I. Uschmann, S. Sebban, G. Grillon, Ph. Balcou, E. Förster, J. P. Geindre, P. Audebert, J. C. Gauthier, and D. Hulin, Nature (London) **410**, 65 (2011).

[41] V. V. Stegailov, Contrib. Plasma Phys. **50**, 31 (2010).

[42] A. Rascon and J. L. Alvarez Rivas, J.Phys. C **16**, 241 (1983).

[43] O. Salminen, P. Riihola, A. Ozols, and T. Viitala, Phys. Rev. B **53**, 6129 (1996).

[44] A. P. Prudnikov, Yu. A. Brychkov, and O. I. Marichev, *Integrals and Series*, Vol. 2: Special functions (Gordon and Breach, New York, 1990).

[45] M. Abramowitz and I. A. Stegun, *Handbook of Mathematical Functions with Formulas, Graphs, and Mathematical Table*, 9th printing (Dover, New York, 1972).

[46] V. V. Uchaikin and V. V. Saenko, Tech. Phys. **46**, 139 (2001).